Rhodium(III) Complexes with Pyridine-2-thiol (pySH) and Pyridine-2-thiolato (pyS) as the only Ligands: Crystal Structures of *mer*-$[Rh(pyS)_3]$, $[Rh(pyS)_2(pySH)_2]Cl{\cdot}0.5H_2O$, and $[Rh(pyS)_3(pySH)]$†

Antony J. Deeming,* Kenneth I. Hardcastle, and M. Nafees Meah
Department of Chemistry, University College London, 20 Gordon Street, London WC1H 0AJ
Paul A. Bates, Helen M. Dawes, and Michael B. Hursthouse*
Department of Chemistry, Queen Mary College, Mile End Road, London E1 4NS

The rhodium(I) compound $[Rh_2Cl_2(CO)_4]$ reacts with an excess of pyridine-2-thiol (pySH) in air to give orange crystals of the oxidised product $[Rh(pyS)_2(pySH)_2]Cl$, the single-crystal *X*-ray structure of which shows two chelating ligands pyS^- in an equatorial plane with mutually *cis* sulphur atoms. The monodentate neutral ligands (pySH) are *trans* co-ordinated through sulphur and are linked through NH ··· Cl^- ··· HN hydrogen bonds to form a large pseudo-chelate ring. The neutral red compound $[Rh(pyS)_3(pySH)]$ is formed only slowly following rapid deprotonation of the cation by basic alumina or NEt_3. The *X*-ray structure shows that a gross stereochemical change has occurred so that two monodentate ligands (pySH and pyS^-) are *cis* while the two chelating ligands (pyS^-) have mutually *trans* sulphur atoms. The deprotonation, with its associated stereochemical change, is reversible. The action of heat on $[Rh(pyS)_3(pySH)]$ gives free pySH and *mer*-$[Rh(pyS)_3]$ (*X*-ray structure reported), which may also be obtained directly from $RhCl_3{\cdot}3H_2O$ and pySH in the presence of base.

The ligand pyridine-2-thiol (pySH) exists predominantly in the 1*H*-pyridine-2-thione form, that is with hydrogen at nitrogen rather than at sulphur,[1] and co-ordinates as such through the sulphur atom in its most common mode of co-ordination (A).[2] It can also co-ordinate as the conjugate anion, pyridine-2-thionate (pyridine-2-thiolato, pyS^-), in the various ways (B)—(E).[3] There appears to be a poor facility to bridge as in (D) compared with the corresponding 2-pyridonato ligand. The compound $[Rh_2Cl_2(\mu\text{-}pyS)_2(pySH)_2(CO)_2]$ is a rare example which we reported that contains bridging pyS^- ligands.[4] The chelating form (C) seems to be much preferred in the sulphur case simply because there is less strain in the four-membered rings containing the larger sulphur atom. For example, there are many examples of four-membered chelate rings with ligands such as dithiocarbamates, thiocarbonates, 1,1-dithiolates *etc.*[5]

Pyridine-2-thionato complexes of rhodium(III) were only known in conjunction with tertiary phosphines prior to our work,[6] but here we will describe rhodium(III) complexes free from other ligands. Tris-chelate complexes of the type $[M(pyS)_3]$ (M = transition metal) are known and the structure of $[NEt_4][Fe^{II}(pyS)_3]$ has been reported.[7] Here we report results on the compounds $[Rh(pyS)_2(pySH)_2]Cl$ and $[Rh(pyS)_3(pySH)]$, as well as the tris-chelate compound $[Rh(pyS)_3]$, their interconversions as summarised in Scheme 1, and their single-crystal *X*-ray structures. Some aspects of this work have been communicated.[8]

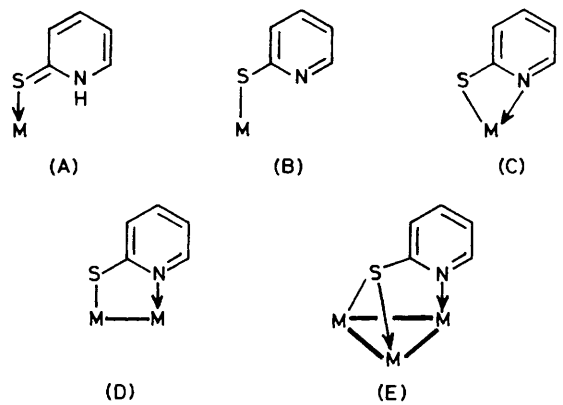

Results and Discussion

Synthesis and Structure of $[Rh(pyS)_2(pySH)_2]Cl$.—Treatment of a chloroform solution of $[Rh_2Cl_2(CO)_4]$ with an excess of pyridine-2-thiol (pySH) gives solutions containing air-sensitive rhodium(I) carbonyl complexes of this ligand. On standing in the absence of air these solutions slowly deposit blue-black crystals of the rhodium(II) dinuclear compound $[Rh_2Cl_2(pyS)_2(pySH)_2(CO)_2]$.[4] However, if air is allowed into solutions of $[Rh_2Cl_2(CO)_4]$ with a ten-told excess of pySH in chloroform, oxidation to rhodium(III) occurs with complete loss of the CO ligands, and over several days pale orange crystals of $[Rh(pyS)_2(pySH)_2]Cl$ are deposited in moderate yield (57%). These may be recrystallised to give crystals suitable for *X*-ray structure determination. Although atmospheric oxygen is required for the formation of this compound, the bubbling of O_2 through the initial solution of pySH and $[Rh_2Cl_2(CO)_4]$ does not appreciably accelerate the reaction or improve the yield.

Compound $[Rh(pyS)_2(pySH)_2]Cl$ is a 1:1 electrolyte [Λ_M = 57 Ω^{-1} cm^2 mol^{-1} at 20 °C in a $MeNO_2$–CH_2Cl_2 mixture (9:1 v/v)]. The ^1H n.m.r. spectrum (Table 1) shows two equally populated ligand environments corresponding to chelating pyS^- and to monodentate S-bonded pySH. Apart from the NH singlet (broad) at δ 13.75, the easiest features of the spectrum to assign are the H^6 signals, which are the lowest-field CH signals. For the chelating pyS^- ligands these appear as doublets but as triplets for the pySH ligands ($J_{H^6H^5} = J_{H^1H^6} = 6.0$ Hz). The observed coupling between NH and the CH^6 (confirmed by

† *mer*-Tris(1*H*-pyridine-2-thionato-*N*,*S*)rhodium(III), bis(1*H*-pyridine-2-thionato-*N*,*S*)bis(1*H*-pyridine-2-thione-*S*)rhodium(III) chloride hydrate (2/1), and (1*H*-pyridine-2-thionato-*S*)bis(1*H*-pyridine-2-thionato-*N*,*S*)(1*H*-pyridine-2-thione-*S*)rhodium(III), respectively.

Supplementary data available: see Instructions for Authors, *J. Chem. Soc., Dalton Trans.*, 1988, Issue 1, pp. xvii—xx.

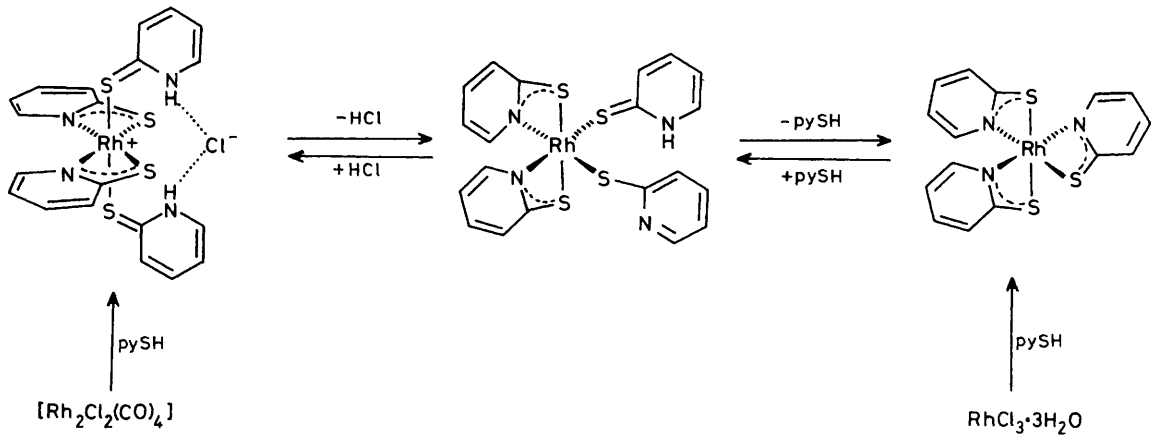

Scheme 1.

Table 1. ^{1}H N.m.r. data (δ) for rhodium(III) complexes containing only pyridine-2-thiol (pySH) and its anion (pyS^-) as ligands[a]

Complex	Chelating pyS	Monodentate pyS or pySH
$[Rh(pyS)_2(pySH)_2]Cl$	8.17 d H^6	13.75 s NH
	6.83 t H^5	8.74 t H^6
	7.40 m H^4	6.96 t H^5
	7.51 d H^3	7.40 t H^4
		6.72 d H^3
$[Rh(pyS)_3(pySH)]$	8.15 d H^6	7.91 d[b] H^6
	6.92 t H^5	6.64 t[b] H^5
	7.30 m H^4	7.30 m[b] H^4
	7.41 d H^3	6.82 d[b] H^3
$[Rh(pyS)_3]$	8.25 m H^6, H^6	
	7.38 m H^6, H^4, H^4, H^4	
	6.80 m H^5, H^3, H^3, H^3	
	6.65 m H^5, H^5	

[a] In $CDCl_3$ at 200 or 400 MHz at room temperature. Multiplicities (d, t, m) indicate approximate appearance of signals. [b] Time-averaged signals for monodentate LH and L (L = pyS) are given in monodentate column.

spin-decoupling experiments) indicates that there is no rapid intermolecular exchange of the NH protons as occurs with the free ligand in solution.

The molecular structure of $[Rh(pyS)_2(pySH)_2]Cl$ is shown in Figure 1; fractional atomic co-ordinates are in Table 2 and selected bond lengths and angles in Table 3. The structure of the cation is approximately C_{2v} with two chelating *cis*-orientated pyS^- ligands in a plane with the monodentate S-bonded pySH ligands *trans*. The overall co-ordination geometry might be considered a skew-trapezoidal bipyramid. Geometries for octahedral complexes with two bidentate ligands in a plane and two monodentate ligands mutually *trans* have been considered and calculations on complexes with bidentate ligands with small bites show that interligand repulsions are minimised when two bidentate ligands distort to form a planar trapezium with the *trans* monodentate ligands skewed together towards the long edge of the trapezium.[9] Quite the reverse is observed for $[Rh(pyS)_2(pySH)_2]Cl$ with the monodentate ligands bent towards the short edge of the trapezium [S(4)–Rh–S(3) = 171.2(1)°]. This is probably not so much a consequence of forces within the complex cation but rather of cation–anion interactions. The *trans* pySH ligands seem to be arranged to maximise H-bonding interactions NH ··· Cl, even though these are not strong as judged by the N–Cl distances [N(4)–Cl 3.156, N(3)–Cl 3.105 Å]. The nitrogen H atoms

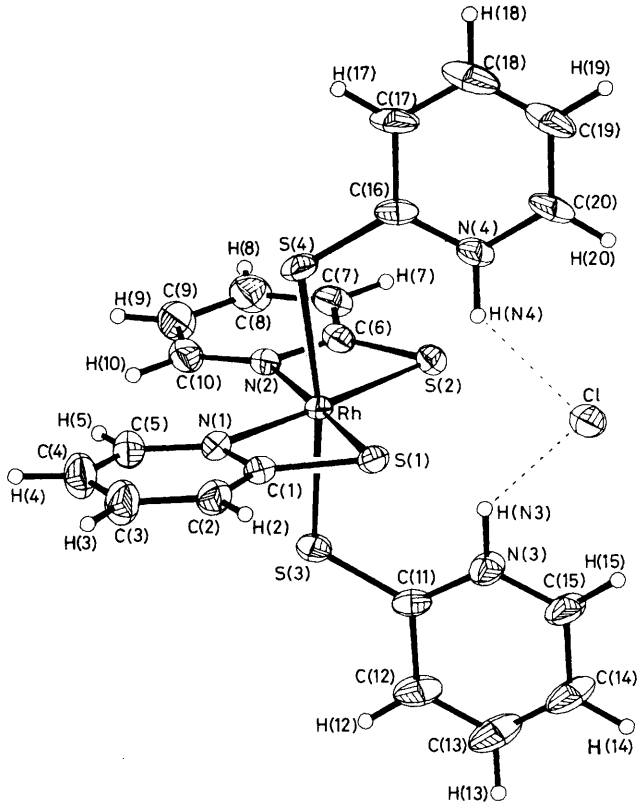

Figure 1. Molecular structure of $[Rh(pyS)_2(pySH)_2]Cl{\cdot}0.5H_2O$

were not located but are in calculated positions in Figure 1. The H bonding creates a large ten-membered chelate ring connecting *trans* sites.

Synthesis and Structure of $[Rh(pyS)_3(pySH)]$.—When a chloroform solution of $[Rh(pyS)_2(pySH)_2]Cl$ is stirred with basic alumina or NEt_3, there is a slow conversion to the neutral dehydrochlorination product $[Rh(pyS)_3(pySH)]$ (90%). In spite of this stoicheiometry, the ^{1}H n.m.r. spectrum is composed of two equal intensity sets of ligand resonances even down to −60 °C. If the overall geometry in the parent cation were maintained on deprotonation, this spectrum could be explained by rapid proton exchange between monodentate ligands pyS^- and pySH. However, if this exchange were rapid it would then be difficult to explain why both the deprotonation of

Table 2. Fractional atomic co-ordinates ($\times 10^4$) for $[Rh(pyS)_2(pySH)_2]Cl\cdot 0.5H_2O$

Atom	*x*	*y*	*z*
Rh	7 032(1)	3 512.6(3)	4 939.4(4)
Cl	6 507(2)	1 376(1)	4 992(2)
S(1)	5 524(2)	2 819(1)	3 704(1)
S(2)	8 306(3)	2 901(1)	6 305(1)
S(3)	9 348(3)	3 497(1)	4 407(2)
S(4)	4 716(3)	3 709(1)	5 435(2)
O(1)	8 801(22)	4 770(8)	−24(13)
N(1)	5 924(8)	4 087(3)	3 788(4)
N(2)	8 290(8)	4 155(3)	5 989(4)
N(3)	9 321(8)	2 132(4)	4 445(5)
N(4)	4 576(8)	2 388(4)	5 843(5)
C(1)	5 113(10)	3 613(4)	3 189(5)
C(2)	4 153(12)	3 793(5)	2 329(6)
C(3)	4 101(16)	4 479(5)	2 090(7)
C(4)	4 892(15)	4 944(5)	2 713(7)
C(5)	5 850(13)	4 736(5)	3 560(6)
C(6)	8 891(10)	3 718(4)	6 680(5)
C(7)	9 818(11)	3 944(5)	7 546(6)
C(8)	10 150(14)	4 622(5)	7 655(7)
C(9)	9 574(15)	5 064(5)	6 933(7)
C(10)	8 630(12)	4 813(5)	6 092(6)
C(11)	9 995(9)	2 706(5)	4 242(5)
C(12)	11 307(10)	2 614(6)	3 858(7)
C(13)	11 835(12)	1 988(7)	3 752(9)
C(14)	11 140(12)	1 423(6)	3 988(8)
C(15)	9 815(12)	1 500(5)	4 344(7)
C(16)	4 099(9)	3 025(5)	5 945(5)
C(17)	3 023(11)	3 118(6)	6 489(6)
C(18)	2 547(13)	2 575(8)	6 894(7)
C(19)	3 061(13)	1 933(8)	6 776(7)
C(20)	4 080(12)	1 845(6)	6 247(7)

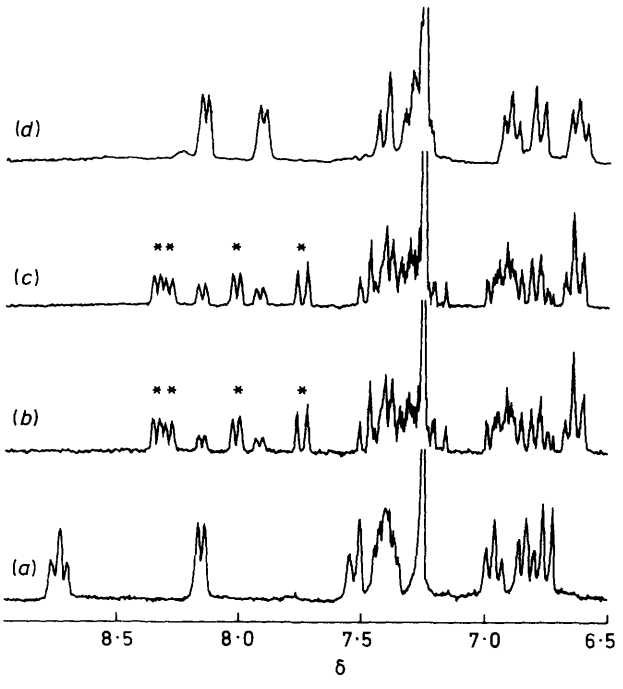

Figure 2. ^1H N.m.r. spectra of $CDCl_3$ solutions of $[Rh(pyS)_2(pySH)_2]Cl$ (*a*), and on the addition of an excess of triethylamine, (*b*) 20 min after the addition, (*c*) 40 min after, and (*d*) after 24 h. Spectra were recorded at room temperature at 200 MHz. The final spectrum (*d*) corresponds to $[Rh(pyS)_3(pySH)]$ while the signals marked * are those of intermediate(s)

Table 3. Selected bond lengths (Å) and angles (°) for the compound $[Rh(pyS)_2(pySH)_2]Cl\cdot 0.5H_2O$

S(1)–Rh	2.380(4)	S(2)–Rh	2.370(4)
S(3)–Rh	2.359(4)	S(4)–Rh	2.360(4)
N(1)–Rh	2.067(8)	N(2)–Rh	2.078(8)
C(1)–Rh	2.694(10)	C(6)–Rh	2.688(11)
C(1)–S(1)	1.741(10)	C(6)–S(2)	1.738(10)
C(11)–S(3)	1.702(11)	C(16)–S(4)	1.712(11)
C(1)–N(1)	1.349(11)	C(5)–N(1)	1.324(12)
C(6)–N(2)	1.338(11)	C(10)–N(2)	1.332(11)
C(11)–N(3)	1.350(11)	C(15)–N(3)	1.343(12)
C(16)–N(4)	1.345(12)	C(20)–N(4)	1.362(12)
C(2)–C(1)	1.373(12)	C(3)–C(2)	1.398(14)
C(4)–C(3)	1.352(15)	C(5)–C(4)	1.372(13)
C(7)–C(6)	1.397(12)	C(8)–C(7)	1.371(14)
C(9)–C(8)	1.372(15)	C(10)–C(9)	1.389(13)
C(12)–C(11)	1.423(13)	C(13)–C(12)	1.342(15)
C(14)–C(13)	1.361(17)	C(15)–C(14)	1.404(14)
C(17)–C(16)	1.415(12)	C(18)–C(17)	1.353(16)
C(19)–C(18)	1.371(18)	C(20)–C(19)	1.355(15)
S(2)–Rh–S(1)	113.7(2)	S(3)–Rh–S(1)	93.4(2)
S(3)–Rh–S(2)	93.2(2)	S(4)–Rh–S(1)	90.8(2)
S(4)–Rh–S(2)	92.2(2)	S(4)–Rh–S(3)	171.2(1)
N(1)–Rh–S(1)	68.8(3)	N(1)–Rh–S(2)	177.2(2)
N(1)–Rh–S(3)	87.7(3)	N(1)–Rh–S(4)	86.6(3)
N(2)–Rh–S(1)	177.4(2)	N(2)–Rh–S(2)	68.7(3)
N(2)–Rh–S(3)	87.3(3)	N(2)–Rh–S(4)	88.2(3)
N(2)–Rh–N(1)	108.7(4)	C(6)–S(2)–Rh	80.2(4)
C(1)–S(1)–Rh	80.0(4)	C(16)–S(4)–Rh	114.4(4)
C(11)–S(3)–Rh	114.0(4)	C(6)–N(2)–Rh	101.6(6)
C(1)–N(1)–Rh	102.1(6)	N(1)–C(1)–S(1)	109.0(6)
C(2)–C(1)–S(1)	130.2(7)	C(2)–C(1)–N(1)	120.8(9)
N(2)–C(6)–S(2)	109.5(7)	C(7)–C(6)–N(2)	120.8(9)
C(7)–C(6)–S(2)	129.6(8)	C(12)–C(11)–N(3)	115.4(9)
N(3)–C(11)–S(3)	123.9(7)	C(12)–C(11)–S(3)	120.7(8)
C(17)–C(16)–S(4)	119.8(9)	C(17)–C(16)–N(4)	117.4(10)
N(4)–C(16)–S(4)	122.8(7)	C(15)–N(3)–H(N3)	116.6(6)
C(11)–N(3)–H(N3)	117.7(5)	C(20)–N(4)–H(N4)	118.6(7)
C(16)–N(4)–H(N4)	118.7(6)		

$[Rh(pyS)_2(pySH)_2]Cl$ and the reprotonation of $[Rh(pyS)_3(pySH)]$ to regenerate the original cation are both quite slow. This was resolved by a single-crystal *X*-ray structure which showed there had been gross structural changes on deprotonation and reprotonation; see later. Figure 2 shows that, after the addition of NEt_3 to $[Rh(pyS)_2(pySH)_2]Cl$, there is an immediate change in the ^1H n.m.r. spectrum. After 20 min no starting material remains and the final form of $[Rh(pyS)_3(pySH)]$ is in low concentration. After 24 h the conversion is essentially complete. The intermediate species of low symmetry, predominating after 20 min, could not be isolated nor its structure assigned from these spectra.

The molecular structure of the deprotonated product, $[Rh(pyS)_3(pySH)]$, is shown in Figure 3. Fractional atomic co-ordinates are given in Table 4 and selected bond lengths and angles in Table 5. The monodentate ligands have moved from mutually *trans* to mutally *cis* positions on deprotonation. All four ligands are different so that an explanation of the ^1H n.m.r. spectrum requires a rapid proton exchange between the nitrogen atoms N(4) and N(3) in solution as well as an intermolecular proton exchange to lose the coupling between H^6 and NH. The monodentate ligand containing S(4) is the pySH ligand. The atom H(4) was located but even without this we could identify this ligand because its geometry is close to those of the monodentate pySH ligands in $[Rh(pyS)_2(pySH)_2]Cl$ and $[Rh_2Cl_2(pyS)_2(pySH)_2(CO)_2]$.[4] Notably, S(4)–C(41) is 1.704(5) Å and the angle Rh–S(4)–C(41) is

115.0(2)°, which may be compared with the corresponding distances and angles in $[Rh(pyS)_2(pySH)_2]Cl$ of 1.702(11) and 1.712(11) Å and 114.0(4) and 114.4(4)° and in $[Rh_2Cl_2(pyS)_2(pySH)_2(CO)_2]$ of 1.719(6) Å and 114.4(3)°.[4] In the other (deprotonated) monodentate ligand the S–C distance is longer [S(3)–C(31) 1.755(5) Å] and the angle at sulphur smaller [Rh–S(3)–C(31) 108.5(2)°]. These changes are as expected if deprotonation involves significant contributions of the forms depicted in Scheme 2. The angle at sulphur changes from one a little less than trigonal planar to one very close to tetrahedral on deprotonation.

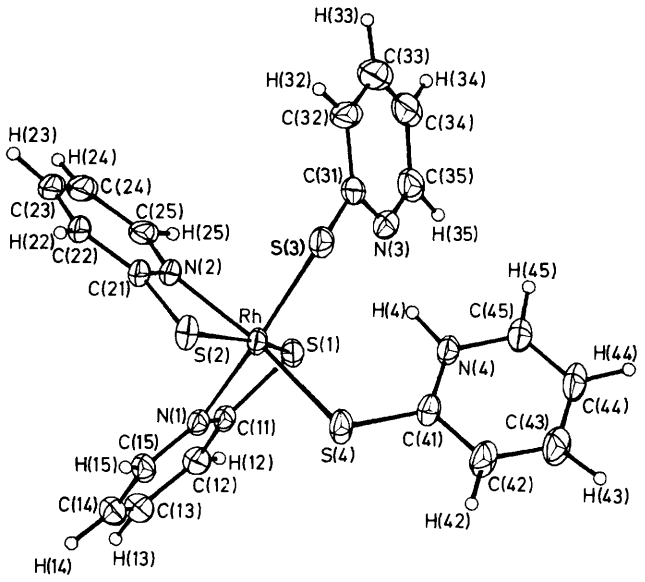

Figure 3. Molecular structure of $[Rh(pyS)_3(pySH)]$

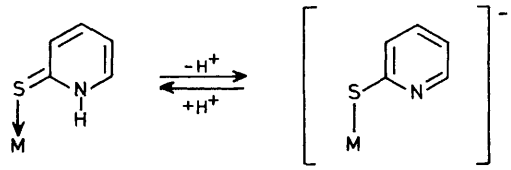

Scheme 2.

Synthesis and Structure of $[Rh(pyS)_3]$.—The electron-impact mass spectra of $[Rh(pyS)_3(pySH)]$ and $[Rh(pyS)_2(pySH)_2]Cl$ do not show parent molecular ions but $[Rh(pyS)_3]^+$ (*m/e* 433) is the highest-mass ion observed. Believing that this ion was the parent molecular ion of a thermal decomposition product of $[Rh(pyS)_3(pySH)]$ and $[Rh(pyS)_2(pySH)_2]Cl$, we melted a sample of $[Rh(pyS)_3(pySH)]$ (m.p. 182 °C) and kept it at this temperature for 5 min. Chromatography of a dichloromethane solution of this material on alumina gave the tris-chelate compound $[Rh(pyS)_3]$ (70%). The ligand pySH sublimed out when $[Rh(pyS)_3(pySH)]$ was heated under vacuum. The ^1H n.m.r. spectrum (Figure 4) can be interpreted in terms of three sets of pyS^- signals which is only consistent with a *mer* configuration; the *fac* configuration would have equivalent ligands. Notable in the spectrum is that one of the H^6 signals (δ 7.4 p.p.m.) is at much higher field than the other two at δ 8.22 and 8.24 p.p.m., which are quite close to corresponding signals in chelating ligands in the other compounds. In the *mer* configuration one of the H^6 protons lies perpendicularly above the plane of another pyS^- ligand and experiences an upfield shift due to the magnetic anisotropy of this other ligand.

The molecular structure of $[Rh(pyS)_3]$ confirming the *mer* configuration is shown in Figure 5. Atomic co-ordinates are given in Table 6 and selected bond lengths and angles in Table 7. We assign the highest-field H^6 signal to that at C(35) which is close to the pyridine ring containing N(21). The co-ordination geometry is octahedral with necessary distortions resulting from the small ligand bite; the N–Rh–S angles within the chelate rings are 69.2(0.5), 69.2(0.5), and 69.5(0.5)°.

Kepert[9] has considered the affect of the small chelate bite on the preference for octahedral *versus* trigonal-prismatic geometry.

Table 4. Fractional atomic co-ordinates (× 10^4) for $[Rh(pyS)_3(pySH)]$

Atom	*x*	*y*	*z*	Atom	*x*	*y*	*z*
Rh	3 774(0.5)	2 816(0.5)	7 789(0.5)	C(42)	6 715(5)	312(3)	8 833(3)
S(1)	1 245(1)	1 158(1)	8 746(1)	C(43)	6 744(5)	−939(4)	8 715(3)
N(1)	2 564(3)	3 489(2)	9 240(2)	C(44)	5 692(5)	−1 823(3)	8 169(3)
C(11)	1 154(4)	2 432(2)	9 632(2)	C(45)	4 647(5)	−1 410(3)	7 774(3)
C(12)	−98(5)	2 488(3)	10 574(2)				
C(13)	89(5)	3 644(3)	11 111(3)	H(12)	−919(38)	1 839(26)	10 798(22)
C(14)	1 522(5)	4 708(3)	10 708(3)	H(13)	−685(43)	3 705(29)	11 707(24)
C(15)	2 748(4)	4 604(3)	9 775(3)	H(14)	1 687(46)	5 466(32)	10 997(25)
S(2)	5 734(1)	4 857(1)	7 004(1)	H(15)	3 671(35)	5 247(25)	9 461(19)
N(2)	2 500(3)	3 667(2)	7 095(2)	H(22)	4 468(43)	6 245(29)	5 780(24)
C(21)	3 822(4)	4 762(3)	6 672(2)	H(23)	1 515(48)	5 714(33)	5 591(27)
C(22)	3 508(7)	5 583(4)	6 067(3)	H(24)	−555(43)	3 985(30)	6 349(25)
C(23)	1 851(8)	5 293(4)	5 941(3)	H(25)	199(37)	2 685(25)	7 219(21)
C(24)	510(7)	4 199(5)	6 400(3)	H(32)	3 333(49)	1 023(33)	4 509(27)
C(25)	880(5)	3 392(4)	6 972(3)	H(33)	1 260(47)	−876(33)	4 259(27)
S(3)	4 814(1)	1 930(1)	6 142(1)	H(34)	−397(50)	−2 375(34)	5 571(27)
N(3)	2 221(4)	−322(2)	6 729(2)	H(35)	431(40)	−1 833(27)	7 064(22)
C(31)	3 104(4)	559(3)	5 952(2)	H(4)	4 011(44)	−14(32)	7 566(25)
C(32)	2 738(6)	363(4)	4 991(3)	H(42)	7 327(44)	875(30)	9 209(24)
C(33)	1 462(7)	−746(5)	4 844(4)	H(43)	7 342(44)	−1 248(31)	9 039(25)
C(34)	512(6)	−1 626(4)	5 640(4)	H(44)	5 719(46)	−2 690(33)	8 008(25)
C(35)	943(6)	−1 364(3)	6 552(3)	H(45)	3 931(38)	−1 941(26)	7 343(21)
S(4)	5 666(1)	2 308(1)	8 541(1)				
N(4)	4 622(3)	−162(2)	7 906(2)				
C(41)	5 635(4)	731(3)	8 413(2)				

In $[Rh(pyS)_3]$ there is a twist of the N(11)S(2)S(3) octahedral face with respect to the opposite S(1)N(21)N(31) face out of the totally staggered to the totally eclipsed configuration by just 16.4°. Thus the compound is roughly 25% distorted from octahedral towards trigonal prismatic; a 60° rotation is necessary for complete transformation.

In the three structures described in this paper Rh–S distances are in the range 2.318—2.396 Å and Rh–N distances in the range 2.034—2.078 Å. There is only a small indication of a *trans* influence, with sulphur having a somewhat higher influence than nitrogen. For example, in $[Rh(pyS)_3]$ the Rh–S distances *trans* to S [2.392(0.5) and 2.383(0.5) Å] are longer than that *trans* to N [2.361(0.5) Å]. Likewise the Rh–N distance *trans* to S [2.050(2) Å] is longer than those *trans* to N [2.034(1) and 2.036(4) Å]. These are small but distinct effects.

Transformations between $[Rh(pyS)_2(pySH)_2]Cl$, $[Rh(pyS)_3(pySH)]$, *and* $[Rh(pyS)_3]$.—Treatment of $[Rh(pyS)_2(pySH)_2]Cl$ with base presumably gives $[Rh(pyS)_3(pySH)]$ with retention of configuration initially with subsequent slow isomerisation to the isolated isomer. This isomerisation is very unlikely to involve pySH dissociation because this would lead to $[Rh(pyS)_3]$ which we have shown to react too slowly with pySH to be an intermediate in this isomerisation. An intramolecular process seems likely: either a trigonal twist or a dissociative mechanism involving chelate ring opening. We believe that the isolated forms of $[Rh(pyS)_2(pySH)_2]Cl$ and $[Rh(pyS)_3(pySH)]$ are thermodynamically in the most stable configurations since they interconvert reversibly *via* unstable configurations.

Since *mer*-$[Rh(pyS)_3]$ is formed at high temperatures by dissociation of pySH from $[Rh(pyS)_3(pySH)]$ or by treatment of $RhCl_3 \cdot 3H_2O$ with pySH, it is probably in its most stable configuration. Prolonged treatment in refluxing toluene gave no change but u.v. photolysis gave partial conversion to another species with new ^1H n.m.r. absorptions in the range δ 6—8. This may be the *fac* isomer but we could not separate this product to confirm this. We have prepared the 6-methyl-substituted derivative of $[Rh(pyS)_3]$ and have shown that this adopts the *fac* configuration but there are clear steric reasons for this.[10]

Experimental

1*H*-Pyridine-2-thione (Aldrich) was used without further purification. $[Rh_2Cl_2(CO)_4]$ was prepared by treating $RhCl_3 \cdot 3H_2O$ with CO (1 atm, 101 325 Pa) in refluxing ethanol. ^1H N.m.r. spectra were recorded in CD_2Cl_2 or $CDCl_3$ on a Varian XL200 spectrometer, i.r. spectra on a Perkin-Elmer PE983 spectrometer, and mass spectra by the University of London Mass Spectra Service at the London School of Pharmacy. Conductivity measurements were on a Philips PR9500 conductivity bridge using shiny Pt electrodes.

Preparation of $[Rh(pyS)_2(pySH)_2]Cl$.—A solution of $[Rh_2Cl_2(CO)_4]$ (0.400 g, 1.03×10^{-3} mol) and pyridine-2-thiol (1.14 g, 1.03×10^{-2} mol) in chloroform (40 cm^3) was stirred under nitrogen for 10 min. The solution was then exposed to air and allowed to stand at room temperature for one week to deposit slowly orange crystals of the product which were washed with diethyl ether and dried under vacuum (0.676 g, 57%). Recrystallisation from a benzene–diethyl ether–chloroform mixture gave yellow-orange crystals (Found: C, 40.3; H, 3.0; Cl, 7.5; N, 9.3. $C_{20}H_{18}ClN_4RhS_4 \cdot 0.1CHCl_3$ requires C, 40.5; H, 3.2; Cl, 7.6; N, 9.4%). Significant i.r. absorptions at 1 575s, 1 132m, 1 022w, and 330.7w cm^{-1} (Nujol). Crystals suitable for *X*-ray structure determination were obtained by slow evaporation of a $MeNO_2$ solution.

Table 5. Selected bond lengths (Å) and angles (°) for the compound $[Rh(pyS)_3(pySH)]$

S(1)–Rh	2.374(3)	N(1)–Rh	2.077(4)
C(11)–Rh	2.698(6)	S(2)–Rh	2.396(3)
N(2)–Rh	2.051(4)	C(21)–Rh	2.684(6)
S(3)–Rh	2.343(3)	S(4)–Rh	2.318(3)
C(11)–S(1)	1.744(5)	C(11)–N(1)	1.354(4)
C(15)–N(1)	1.339(4)	C(12)–C(11)	1.374(5)
C(13)–C(12)	1.379(5)	C(14)–C(13)	1.371(6)
C(15)–C(14)	1.368(5)	C(21)–S(2)	1.738(5)
C(21)–N(2)	1.359(4)	C(25)–N(2)	1.333(5)
C(22)–C(21)	1.387(5)	C(23)–C(22)	1.363(7)
C(24)–C(23)	1.377(7)	C(25)–C(24)	1.373(6)
C(31)–S(3)	1.755(5)	C(31)–N(3)	1.341(5)
C(35)–N(3)	1.338(5)	C(32)–C(31)	1.384(5)
C(33)–C(32)	1.368(7)	C(34)–C(33)	1.362(7)
C(35)–C(34)	1.347(6)	C(41)–S(4)	1.704(5)
C(41)–N(4)	1.343(5)	C(45)–N(4)	1.362(5)
H(4)–N(4)	0.831(33)	C(42)–C(41)	1.391(5)
C(43)–C(42)	1.365(6)	C(44)–C(43)	1.388(6)
C(45)–C(44)	1.341(6)		
N(1)–Rh–S(1)	69.0(2)	S(2)–Rh–S(1)	163.1(1)
S(2)–Rh–N(1)	98.5(2)	N(2)–Rh–N(1)	89.1(2)
N(2)–Rh–S(1)	98.5(2)	N(2)–Rh–S(2)	69.2(2)
S(3)–Rh–N(1)	173.5(1)	S(3)–Rh–S(1)	105.9(1)
S(3)–Rh–S(2)	85.6(1)	S(3)–Rh–N(2)	87.6(2)
S(4)–Rh–N(1)	89.4(2)	S(4)–Rh–S(1)	92.7(1)
S(4)–Rh–S(2)	98.6(1)	S(4)–Rh–N(2)	167.3(1)
S(4)–Rh–S(3)	95.0(1)	C(11)–N(1)–Rh	101.6(3)
C(11)–S(1)–Rh	80.3(2)	C(15)–N(1)–C(11)	119.8(3)
C(15)–N(1)–Rh	138.4(2)	N(1)–C(11)–S(1)	109.1(3)
C(12)–C(11)–S(1)	130.1(2)	C(21)–N(2)–Rh	101.9(3)
C(21)–S(2)–Rh	79.2(2)	C(25)–N(2)–C(21)	121.0(4)
C(25)–N(2)–Rh	137.0(2)	N(2)–C(21)–S(2)	109.6(3)
C(22)–C(21)–S(2)	130.7(3)	C(22)–C(21)–N(2)	119.7(4)
C(31)–S(3)–Rh	108.5(2)	C(32)–C(31)–S(3)	120.1(4)
N(3)–C(31)–S(3)	119.2(3)	C(41)–S(4)–Rh	115.0(2)
H(4)–N(4)–C(45)	110.9(25)	H(4)–N(4)–C(41)	125.3(25)
C(42)–C(41)–S(4)	120.2(3)	N(4)–C(41)–S(4)	123.5(3)

Table 6. Fractional atomic co-ordinates ($\times 10^4$) for $[Rh(pyS)_3]$

Atom	*x*	*y*	*z*
Rh	938(0.5)	796(0.5)	3 121(0.5)
S(1)	11(1)	2 471(0.5)	2 357(0.5)
S(2)	2 449(1)	−478(0.5)	4 073(0.5)
S(3)	−1 037(1)	155(1)	3 486(0.5)
C(11)	774(2)	2 910(1)	3 611(1)
C(12)	832(2)	3 951(2)	4 062(2)
C(13)	1 508(2)	4 082(2)	5 091(2)
C(14)	2 128(2)	3 199(2)	5 649(2)
C(15)	2 039(2)	2 184(2)	5 169(2)
N(11)	1 367(1)	2 053(1)	4 171(1)
C(21)	3 450(2)	272(2)	3 412(1)
C(22)	4 787(2)	252(2)	3 502(2)
C(23)	5 337(2)	972(2)	2 900(2)
C(24)	4 582(2)	1 706(2)	2 226(2)
C(25)	3 268(2)	1 716(2)	2 182(2)
N(21)	2 727(1)	1 006(1)	2 760(1)
C(31)	−985(2)	−570(2)	2 332(2)
C(32)	−1 869(2)	−1 303(2)	1 760(2)
C(33)	−1 581(3)	−1 778(2)	860(2)
C(34)	−436(3)	−1 527(2)	549(2)
C(35)	416(2)	−801(1)	1 147(2)
N(31)	124(2)	−327(1)	2 015(1)

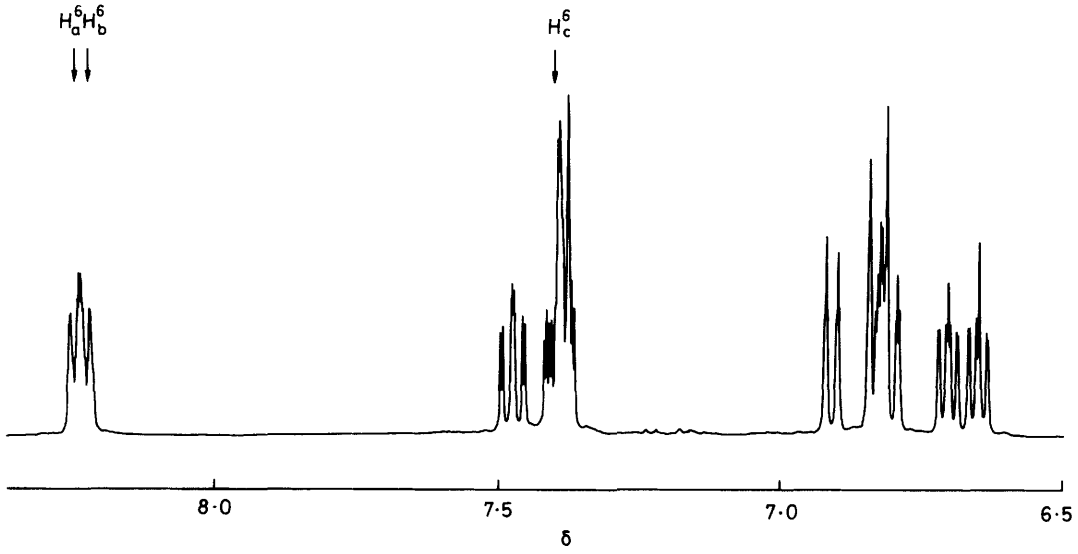

Figure 4. ^1H N.m.r. spectrum of *mer*-[Rh(pyS)$_3$] in $CDCl_3$ at 400 MHz at room temperature; the large differences in δ for the signals for H_a^6, H_b^6, and H_c^6 for the three different pyS ligands are indicated

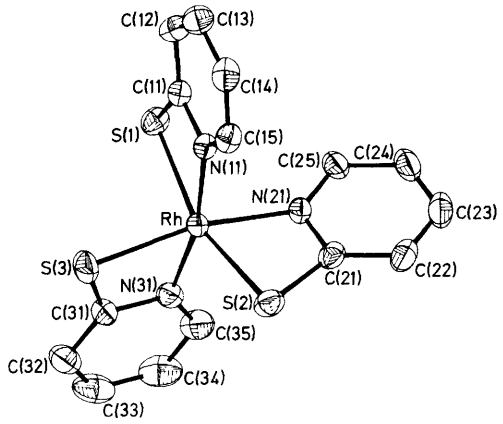

Figure 5. Molecular structure of [Rh(pyS)$_3$] with H atoms omitted for clarity

Preparation of [Rh(pyS)$_3$(pySH)].—The salt [Rh(pyS)$_2$(pySH)$_2$]Cl (0.100 g, 1.72 × 10^{-4} mol) was dissolved in a minimum volume of hot chloroform. Alumina (2 g) was added to the solution and the mixture stirred for 2 h. The deep red solution was concentrated to *ca.* 10 cm^3 and eluted through a 5% deactivated neutral alumina column with chloroform. The product was isolated as a red solid and crystallised from a chloroform–benzene–diethyl ether mixture to give deep red crystals (0.089 g, 90%), m.p. 182 °C, suitable for *X*-ray structure determination (Found: C, 44.05; H, 3.1; N, 10.3. $C_{20}H_{17}N_4RhS_4$ requires C, 44.05; H, 3.1; N, 10.0%). Significant i.r. absorptions: 1 577s, 1 258m, 484m, 453w, and 316w cm^{-1} (Nujol).

The complex [Rh(pyS)$_3$(pySH)] was also prepared by adding NEt_3 (2 mol per mol Rh) to a solution of [Rh(pyS)$_2$(pySH)$_2$]Cl in $CDCl_3$ in an n.m.r. tube. The reaction required 24 h to go to completion.

Preparation of [Rh(pyS)$_3$].—(*a*) Crystals of [Rh(pyS)$_3$(pySH)] (0.050 g, 9.2 × 10^{-5} mol) were heated gently in a porcelain crucible until molten. The melt was cooled, dissolved in dichloromethane, and eluted through a 5% deactivated alumina column. The product was crystallised from a chloroform–benzene–light petroleum (b.p. 30—40 °C) mixture to give ruby red crystals (0.028 g, 70%). (*b*) A solution of $RhCl_3 \cdot 3H_2O$ (0.200 g, 7.59 × 10^{-4} mol), pyridine-2-thiol (0.506 g, 4.55 × 10^{-3} mol), and sodium ethoxide (10 cm^3 of a 0.4 mol dm^{-3} solution in ethanol) was heated under reflux for 9 h. The solution was filtered through sand and Celite and the solvent removed under reduced pressure. The residue was suspended in dichloromethane, filtered, and the filtrate eluted

Table 7. Selected bond lengths (Å) and angles (°) for the compound [Rh(pyS)$_3$]

S(1)–Rh	2.392(0.5)	S(2)–Rh	2.383(0.5)
S(3)–Rh	2.361(0.5)	N(11)–Rh	2.034(1)
N(21)–Rh	2.050(2)	N(31)–Rh	2.036(4)
C(11)–S(1)	1.735(4)	C(12)–C(11)	1.393(4)
N(11)–C(11)	1.350(2)	C(13)–C(12)	1.380(4)
C(14)–C(13)	1.385(4)	C(15)–C(14)	1.378(4)
N(11)–C(15)	1.345(3)	C(21)–S(2)	1.743(4)
C(22)–C(21)	1.394(4)	N(21)–C(21)	1.354(3)
C(23)–C(22)	1.374(5)	C(24)–C(23)	1.382(4)
C(25)–C(24)	1.378(4)	N(21)–C(25)	1.340(3)
C(31)–S(3)	1.737(4)	C(32)–C(31)	1.393(4)
N(31)–C(31)	1.348(3)	C(33)–C(32)	1.380(5)
C(34)–C(33)	1.381(5)	C(35)–C(34)	1.382(4)
N(31)–C(35)	1.346(3)		
S(2)–Rh–S(1)	161.0(0.5)	S(3)–Rh–S(1)	93.4(0.5)
S(3)–Rh–S(2)	102.1(0.5)	N(11)–Rh–S(1)	69.2(0.5)
N(11)–Rh–S(2)	96.6(0.5)	N(11)–Rh–S(3)	101.9(0.5)
N(21)–Rh–S(1)	96.9(0.5)	N(21)–Rh–S(2)	69.2(0.5)
N(21)–Rh–S(3)	167.8(0.5)	N(31)–Rh–S(1)	102.0(0.5)
N(31)–Rh–S(2)	93.7(0.5)	N(31)–Rh–S(3)	69.5(0.5)
N(21)–Rh–N(11)	87.8(2)	N(31)–Rh–N(11)	167.8(1)
N(31)–Rh–N(21)	101.9(2)	C(12)–C(11)–S(1)	129.9(2)
C(11)–S(1)–Rh	78.9(2)	N(11)–C(11)–C(12)	120.5(3)
N(11)–C(11)–S(1)	109.6(2)	C(11)–N(11)–Rh	102.3(2)
C(15)–N(11)–Rh	136.6(1)	C(21)–S(2)–Rh	79.4(2)
C(22)–C(21)–S(2)	130.8(2)	N(21)–C(21)–S(2)	109.1(2)
N(21)–C(21)–C(22)	120.0(3)	C(21)–N(21)–Rh	102.0(2)
C(25)–N(21)–Rh	136.1(1)	C(32)–C(31)–S(3)	130.2(2)
C(31)–S(3)–Rh	79.6(2)	N(31)–C(31)–C(32)	120.9(3)
N(31)–C(31)–S(3)	108.9(2)	C(31)–N(31)–Rh	102.0(2)
C(35)–N(31)–Rh	137.1(1)	C(35)–N(31)–C(31)	120.8(3)

through an alumina column. The product was crystallised from a chloroform–benzene–light petroleum (b.p. 30—40 °C) mixture to give ruby red crystals (0.140 g, 43%) (Found: C, 40.9; H, 2.75; N, 9.4. $C_{15}H_{12}N_3RhS_3 \cdot 0.1CHCl_3$ requires C, 40.7; H, 2.7; N, 9.4%). Parent molecular ion observed at 433 relative molecular mass.

Reactions monitored by ^{1}H *N.M.R. Spectra.*—*[Rh(pyS)$_3$] with pyridine-2-thiol.* A solution of [Rh(pyS)$_3$] (0.050 g, 1.15×10^{-4} mol) and pyridine-2-thiol (0.026 g, 2.3×10^{-4} mol) in toluene (10 cm^3) was refluxed for 12 h. After removal of the solvent, the ^{1}H n.m.r. spectrum in $CDCl_3$ showed the formation of [Rh(pyS)$_3$(pySH)] (44% conversion).

[Rh(pyS)$_3$] *with pyridine-2-thiol and* HCl. A solution of [Rh(pyS)$_3$] (0.050 g, 1.15×10^{-4} mol) and pyridine-2-thiol (0.026 g, 2.3×10^{-4} mol) in 2-methoxyethanol (10 cm^3) was refluxed for 12 h. The solvent was removed and the residue dissolved in $CDCl_3$ and treated with an excess of HCl. The ^{1}H n.m.r. spectrum showed a 36% conversion to [Rh(pyS)$_2$(pySH)$_2$]Cl.

[Rh(pyS)$_3$(pySH)] *with* HCl. A solution of HCl in dichloromethane (0.35 cm^3 of a 0.128 mol dm^{-3} solution) was added to a solution of [Rh(pyS)$_3$(pySH)] (0.025 g, 4.6×10^{-5} mol) in dry dichloromethane (5 cm^3) and stirred overnight at room temperature. The solvent was removed and the residue dissolved in $CDCl_3$. The ^{1}H n.m.r. spectrum showed it to be predominantly [Rh(pyS)$_2$(pySH)$_2$]Cl (90%). Other species in low concentration were apparent from H^6 resonances at δ 8.29 and 8.00.

Crystallographic Studies.—*Crystal data.* [Rh(pyS)$_2$(pySH)$_2$]Cl·0.5H$_2$O (**1**): $C_{20}H_{18}ClN_4RhS_4 \cdot 0.5H_2O$, M = 588.2, monoclinic, a = 8.654(4), b = 19.753(3), c = 15.045(3) Å, β = 106.41(3)°, U = 2 466.9 Å^3, space group $P2_1/n$, Z = 4, D_c = 1.58 g cm^{-3}, F(000) = 1 184, λ = 0.710 69 Å, μ(Mo-K_α) = 10.8 cm^{-1}.

[Rh(pyS)$_3$(pySH)] (**2**): $C_{20}H_{17}N_4RhS_4$, M = 542.7, triclinic, a = 8.278(1), b = 10.901(2), c = 13.312(4) Å, α = 95.26(2), β = 72.38(2), γ = 108.85(1)°, U = 1 083.5 Å^3, space group $P\bar{1}$, Z = 2, D_c = 1.66 g cm^{-3}, F(000) = 546, λ = 0.710 69 Å, μ(Mo-K_α) = 10.9 cm^{-1}.

[Rh(pyS)$_3$] (**3**): $C_{15}H_{12}N_3RhS_3$, M = 431.5, monoclinic, a = 10.563(1), b = 12.205(1), c = 12.846(1) Å, β = 101.53(1)°, U = 1 622.7 Å^3, space group $P2_1/n$, Z = 4, D_c = 1.77 g cm^{-3}, F(000) = 860, λ = 0.710 69 Å, μ(Mo-K_α) = 13.2 cm^{-1}.

Data collections. Unit-cell parameters and intensity data, for all structures, were obtained by following previously detailed procedures,[11] using a CAD4 diffractometer operating in the ω–2θ scan mode, with graphite monochromated Mo-K_α radiation. A total of 4 783 unique reflections were collected for (**1**) ($1.5 \leqslant \theta \leqslant 25°$), 3 805 for (**2**) ($1.5 \leqslant \theta \leqslant 25°$), and 4 281 for (**3**) ($1.5 \leqslant \theta \leqslant 28°$). The reflection intensities were corrected for absorption using the azimuthal-scan method;[12] maximum and minimum transmission factors: (**1**), 1.00 and 0.87; (**2**), 1.00 and 0.96; (**3**), 1.00 and 0.92.

Solution and refinement of structures. All structures were solved by the application of routine heavy-atom methods, and refined by full-matrix least squares (SHELX 76[13]). Towards the end of the refinement for (**1**) a single isolated peak was located in a difference Fourier synthesis. This was assumed to belong to a disordered water molecule and was refined as such in all subsequent calculations (occupancy factor 0.5). All non-hydrogen atoms for (**1**), (**2**), and (**3**) were refined with anisotropic thermal coefficients. The final cycle of refinement included all located hydrogen atoms for (**2**) and (**3**) (isotropically refined), while those of (**1**) were placed into calculated positions (C–H and N–H 0.98 Å, U = 0.10 Å^2). The final values of R and R' were: (**1**), 0.049 and 0.054; (**2**), 0.024 and 0.022; (**3**), 0.021 and 0.022. The total number of variables refined and data used were: (**1**), 280 variables, 3 398 data [$F_o \geqslant 6\sigma(F_o)$]; (**2**), 330 variables, 3 295 data [$F_o \geqslant 3\sigma(F_o)$]; (**3**), 248 variables, 3 532 data [$F_o \geqslant 3\sigma(F_o)$]. The function minimised in each case was $\Sigma w(|F_o| - |F_c|)^2$, with weights $1/[\sigma^2(F_o)]$. Final difference maps, one for each of the three structures, were featureless. Atomic scattering factors and anomalous scattering parameters were taken from refs. 14 and 15 respectively. All computations were made on a DEC VAX-11/750 computer.

Acknowledgements

We thank University College London for a studentship (for M. N. M.), California State University at Northridge for leave of absence (for K. I. H.), the S.E.R.C. for support of the crystallographic work, and Johnson-Matthey Ltd. for a loan of rhodium trichloride.

References

1 A. Albert and G. B. Barlin, *J. Chem. Soc.*, 1959, 2384.
2 B. P. Kennedy and A. B. P. Lever, *Can. J. Chem.*, 1972, **50**, 3488; E. Binamira-Soriaga, M. Lundeen, and K. Seff, *Acta Crystallogr., Sect. B*, 1979, **35**, 2875.
3 P. Mura, B. G. Olby, and S. D. Robinson, *J. Chem. Soc., Dalton Trans.*, 1985, 2384 and refs. therein; I. Kinoshita, Y. Yasuba, K. Matsumoto, and S. Ooi, *Inorg. Chim. Acta*, 1983, **80**, L13.
4 A. J. Deeming, M. N. Meah, H. M. Dawes, and M. B. Hursthouse, *J. Organomet. Chem.*, 1986, **299**, C25.
5 R. P. Burns, F. P. McCullough, and C. A. McAuliffe, *Adv. Inorg. Chem. Radiochem.*, 1980, **23**, 211 and refs. therein.
6 R. W. Mitchell, J. D. Ruddick, and G. Wilkinson, *J. Chem. Soc. A*, 1971, 3224.
7 S. G. Rosenfield, S. A. Swedberg, S. K. Arora, and P. K. Mascharak, *Inorg. Chem.*, 1986, **25**, 2109.
8 A. J. Deeming and M. N. Meah, *Inorg. Chim. Acta*, 1986, **117**, L13.
9 D. L. Kepert, *Prog. Inorg. Chem.*, 1977, **23**, 1.
10 A. J. Deeming and N. M. Meah, unpublished work.
11 M. B. Hursthouse, R. A. Jones, K. M. A. Malik, and G. Wilkinson, *J. Am. Chem. Soc.*, 1979, **101**, 4128.
12 A. C. T. North, D. C. Phillips, and F. S. Mathews, *Acta Crystallogr., Sect. A*, 1968, **24**, 351.
13 G. M. Sheldrick, SHELX 76, Program for crystal structure determination and refinement, University of Cambridge, 1976.
14 D. T. Cromer and J. B. Mann, *Acta Crystallogr., Sect. A*, 1968, **24**, 321.
15 D. T. Cromer and D. Liberman, *J. Chem. Phys.*, 1970, **53**, 1891.

Received 7th January 1987; *Paper* 7/035